Medical & Biological Engineering & Computing
https://doi.org/10.1007/s11517-022-02516-0

ORIGINAL ARTICLE

Study of the significance of parameters and their interaction on assessing femoral fracture risk by quantitative statistical analysis

Rabina Awal[1] · Jalel Ben Hmida[1] · Yunhua Luo[2] · Tanvir Faisal[1]

Received: 10 January 2021 / Accepted: 21 January 2022

Abstract
Early assessment of hip fracture helps develop therapeutic and preventive mechanisms that may reduce the occurrence of hip fracture. An accurate assessment of hip fracture risk requires proper consideration of the loads, the physiological and morphological parameters, and the interactions between these parameters. Hence, this study aims at analyzing the significance of parameters and their interactions by conducting a quantitative statistical analysis. A multiple regression model was developed considering different loading directions during a sideways fall (angle (α) and (β) on the coronal and transverse planes, respectively), age, gender, patient weight, height, and femur morphology as independent parameters and Fracture Risk Index (FRI) as a dependent parameter. Strain-based criteria were used for the calculation of FRI with the maximum principal strain obtained from quantitative computed tomography–based finite element analysis. The statistical result shows that β ($p < 0.0000$), age ($p < 0.0006$), true moment length ($p < 0.0006$), gender ($p < 0.0015$), FNA ($p < 0.0213$), height ($p < 0.0238$), and FSL ($p < 0.0315$) significantly affect FRI where β is the most influential parameter. The significance of two-level interaction ($p < 0.05$) and three-level interaction ($p < 0.05$) shows that the effect of parameters is dissimilar and depends on other parameters suggesting the variability of FRI from person to person.

Keywords Hip fracture · Finite element analysis · Multiple regression analysis · Parametric quantitative analysis

1 Introduction

Hip fracture—a traumatic injury—has a significant impact on the economy as well as quality of life. With an increase in life expectancy and a growing population of the elderly, a higher number of hip fractures can be anticipated as well as the consequent social and economic burden on the USA and other countries worldwide [1]. An early assessment of hip fracture is especially effective in preventing hip fracture of the elderly people. Nearly 1.66 million cases are reported each year and this number is predicted to increase fourfold by 2050 according to the World Health Organization (WHO) [2]. It was reported that about 20% of orthopedic beds in the USA are typically occupied by patients with hip fractures where the mortality rate is one in five within the first year of hip surgery [3]. Hip fracture is considered a common injury that affects more than 75 million people in the USA, Europe, and Asia [4]. One of the major causes of hip fracture is osteoporosis. According to WHO, osteoporosis, clinically defined as the loss of bone mineral density (BMD), causes more than 8.9 million fractures annually among which 4.5 million occur in the USA and Europe alone [5] and an estimated cost of annual osteoporotic fracture treatment in the USA alone is $13.8 billion [6]. Although osteoporosis [7] is considered the primary cause of hip fracture, other factors such as gender, weight, height, bone morphology, and, above all, the magnitude and direction of load due to fall contribute to the fracture. Therefore, a comprehensive quantitative analysis of the parameters influencing the hip fracture is necessary to evaluate the categorical parametric impact on hip fracture, and thereby identifying critical parameters that may dominate femoral fracture.

Clinically, early prediction of osteoporotic hip fracture is done by measuring BMD using dual-energy X-ray absorptiometry (DXA) and is represented by a *T*-score, which is compared against the standard range of values defined by WHO [5, 8]. However, densitometry analysis measures

✉ Tanvir Faisal
tanvir.faisal@louisiana.edu

[1] Department of Mechanical Engineering, University of Louisiana at Lafayette, Lafayette, LA, USA

[2] Department of Mechanical Engineering, University of Manitoba, Winnipeg, MB, Canada

Published online: 04 February 2022

BMD via 2D projection of CT images which may lead to underestimation or overestimation of BMD depending on the size of bone [9]. Besides, it does not consider the 3D bone morphology. To consider structural and geometric parameters along with BMD, hip structural analysis (HSA) has been used to predict the fracture risk [8, 10–12] considering the femoral neck as a simple cantilever beam structure [12–14]. The assumption of classical beam theory makes HSA oversimplified especially in the femoral neck (FN) and intertrochanteric (ITC) regions. Integrating medical imaging technologies such as DXA and quantitative computed tomography (QCT) with finite element analysis (FEA) can assess the fracture risk more accurately in comparison with bone densitometry and diagnostic imaging only [15–17], and the QCT-based FEA is more effective as it considers bone material properties (i.e., BMD), bone anatomy, and loading variability [18].

Traditionally, decrease in BMD over time indicates a higher probability of osteoporotic fragile fracture. Typically, between the ages of 25 and 29, BMD in the femur is in the maximum range [2], which declines with increasing age; and therefore, a low BMD is prevalent in elderly people. In addition, dissimilar BMD loss is also observed between female and male due to the different rates of BMD loss [19]. This uneven BMD declination rate results in an unequal probability of osteoporotic fracture such that the tendency of hip fracture is 21.3% for female and 5.5% for male [19, 20], resembling gender as an important factor. However, neither BMD nor gender is the sole criteria to influence the fractures within the same gender and age group, respectively [21–24]. Furthermore, prior studies show that 90% of hip fractures occur due to simple fall [25, 26], explicitly indicating the impact of load magnitude. Pinilla et al. [25] further showed that a change in loading direction from 0° to 30° measured from the femoral neck axis on a transverse plane resulted in a decrease in failure load by 24%, which is comparable to 25 years of age-related bone loss. The variation of loading angle from 0° to 45° measured from the femoral neck axis reduced the structural capacity of a femur by 26%, which is equivalent to 2–3 decades of bone loss as well [26]. Femur geometry also plays an important role in femoral fracture [27]. Although hip fracture is influenced by several parameters cumulatively, prior works considered isolated effects of those parameters. Therefore, the goal of this work is to assess the hip fracture risk combining patient physiology, bone morphology, and the mechanics of fall.

Prior studies discretely investigated the importance of factors such as loading direction, bone density, bone morphology, and age on femur strength [25, 26, 28, 29], which fail to directly correlate fracture risk. Furthermore, the level of significance of the associated parameters is yet to be analyzed. Therefore, in addition to QCT-based FEA, we opted for quantitative statistical analysis to investigate the effect of parameters and their level of significance. In this regard, along with the magnitude of fall load, loading directions represented by angle α on the coronal plane and angle β on the transverse plane were considered to mimic various sideways fall postures. In addition, age, gender, patient height, weight, and femoral morphology were considered in the present study as the most crucial parameters based on their clinical relevance [2, 25–27, 30]. A multiple regression model was considered to measure the degree to which the parameters as independent variables are related to fracture risk index (FRI)—the dependent parameter [31]—which is defined as the ratio of maximum strain to allowable strain. The independent parameters were also ranked to identify the most critical ones that impact the hip fracture. We further investigated the dependence of parameters to analyze how the effect of one parameter depends on another—a crucial aspect of fracture assessment that is rarely explored. Hence, this study explores how intensely a femoral (hip) fracture is affected by the physiological and morphological parameters along with loading effects and their relative importance according to their extent of the effect.

2 Materials and method

QCT images of 30 anonymous adults, removing all personal information, were considered in this work. The average age, height, and weight of the patients were 64.8 ± 8.86 years, 157.49 ± 6.66 cm, and 82.9 ± 14.53 kg, respectively. The average length of a femur was 43.9 ± 2.3 cm, and the length and width of the femoral neck were 11.4 ± 7.53 cm and 3.5 ± 0.4 cm, respectively, with a neck angle of 35.8°± 12.22°. The CT dataset of the patients in Digital Imaging and Communications in Medicine (DICOM) format were obtained from the Great-West Life PET/CT Center located at the Health Science Center in Winnipeg, Canada [18, 28].

2.1 Image acquisition using CT scan

CT scanned images were obtained by a SIEMENS S5VB40B CT scan machine (Siemens Medical Solution, Malvern, USA) with acquisition and reconstruction parameters of 120 kVp and 244 mAs, respectively, and image matrix of 512×512 pixels. A calcium hydroxyapatite calibration phantom (Mindways Inc., Austin, TX, USA) was mounted during the time of imaging for an accurate estimation of BMD, correcting the scanner drift. The clinical dataset was acquired in two series, one with slices thickness of 3 mm and another one with 1.5 mm, following the center's imaging protocol. In the current work, we constructed the 3D femur geometry from the high-resolution dataset with a slice thickness 1.5 mm.

2.2 Image processing and FE model generation

Using the medical image processing software Mimics® 16.0 (Materialise N.V., Leuven, Belgium), the 3D femur geometry was reconstructed after carefully segmenting the femur from the pelvis, tibial part, fat, and muscle along with other operations like dilation and erosion to have a smooth bone surface. During the image processing steps, the 2D images obtained from the CT scanner were stacked together to get the 3D geometry using the inbuilt interpolation algorithm in Mimics. The number of slices/2D images vary among the patients ranging from 511 to 585, depending on patients' height. The reconstructed femur was meshed with 4-node tetrahedral elements using the mesh processing tools of Mimics. A maximum edge length of 3.4 mm was determined from the convergence test, achieved when the displacement between the two successive iterations fell within 5%, where the displacement of a predetermined point (node) was compared against the maximum element size keeping the same boundary and loading conditions. Poisson's ratio was assumed to be 0.4 for all directions [18].

2.3 Inhomogeneous material distributions

Although bone is anisotropic [32, 33], isotropic and inhomogeneous material distributions have sufficient adequacy to conduct FEA to accurately predict the stress and strain in the femur [21, 31, 33, 34], and were adopted in this work. Each voxel of DICOM images was correlated with the bone density expressed in Hounsfield Unit (HU). According to our prior work [18, 28, 35], we considered 50 material bins for the inhomogeneous material distributions in the femur. The modulus of elasticity (E) was calculated based on the empirical Eqs. (1) and (2) [33, 35, 36].

$$\rho_{ash} = 0.04126 + 0.000854 \times HU \left(g\, cm^{-3}\right) \tag{1}$$

$$E = 10500 \times \rho_{ash}^{2.29} \, (MPa) \tag{2}$$

where HU is the Hounsfield unit, ρ_{ash} is the ash density, and E is the modulus of elasticity.

2.4 Loading and boundary conditions

The sideways falling postures were imitated by the different loading directions acted onto the greater trochanter during a range of possible falling scenarios [28]. The load was distributed to the medial side on the superior surface of the femoral head. The distal condyle of the femur was completely fixed from both translation and rotation in all 3 directions [25, 26, 31, 37–41], and the greater trochanter was fixed along the loading direction only [3]. The magnitude of load, representing the sideways fall from standing height, P_{fall}, is estimated by [35],

$$P_{fall} = 8.25 \times w \times \left(\frac{h}{170}\right)^{1/2} (N) \tag{3}$$

where w and h are the weight and height of a patient, respectively.

The fixed boundary conditions were primarily chosen based on ex vivo/in vitro experiments, where the femur bone (cadaveric/synthetic sawbone) is usually constrained from translation and rotation. Table 1 summarizes the FE modeling parameters considered in the present study. To accommodate the variations of sideways fall postures (denoted by orientations herein), P_{fall} was varied from the shaft axis on the coronal plane (α) and from the femoral neck axis on the transverse plane (β) (Fig. 1). The sideways fall configurations denoted by sw 1 to sw 4 represent the variation of α from 0° to 120° at 30° interval, fixing angle β at 0° (Fig. 2a). On the other hand, the configurations sw 5 to sw 7 represent the variation of β from 15° to 45° in an interval of 15°, keeping α constant at 120° (Fig. 2b). Because of the reaction force on femoral head

Table 1 Parameters considered in the FE simulation

Materials	Isotropic and inhomogeneous
Number of materials bins	50
Element type	4-node tetrahedral element
Boundary condition (BC)	
Distal end	Fixed
Greater trochanter	Fixed on loading direction
Femoral head	Load applied

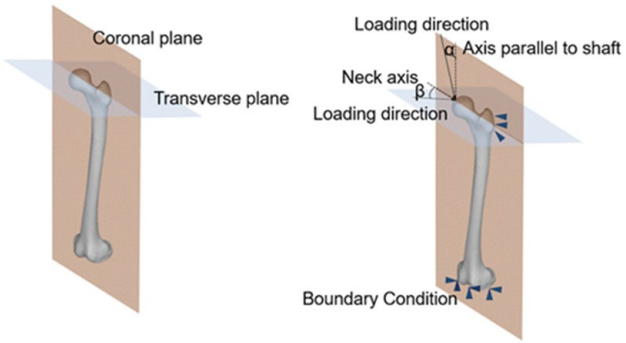

Fig. 1 Loading and boundary conditions. The distal condyle of the femur was fixed in all direction, greater trochanter was fixed in loading direction, and load was applied on femoral head from different directions, α and β. α is the angle made by the loading direction on coronal plane with respect to shaft axis, and β is the angle made by the loading direction on transverse plane with respect to neck axis

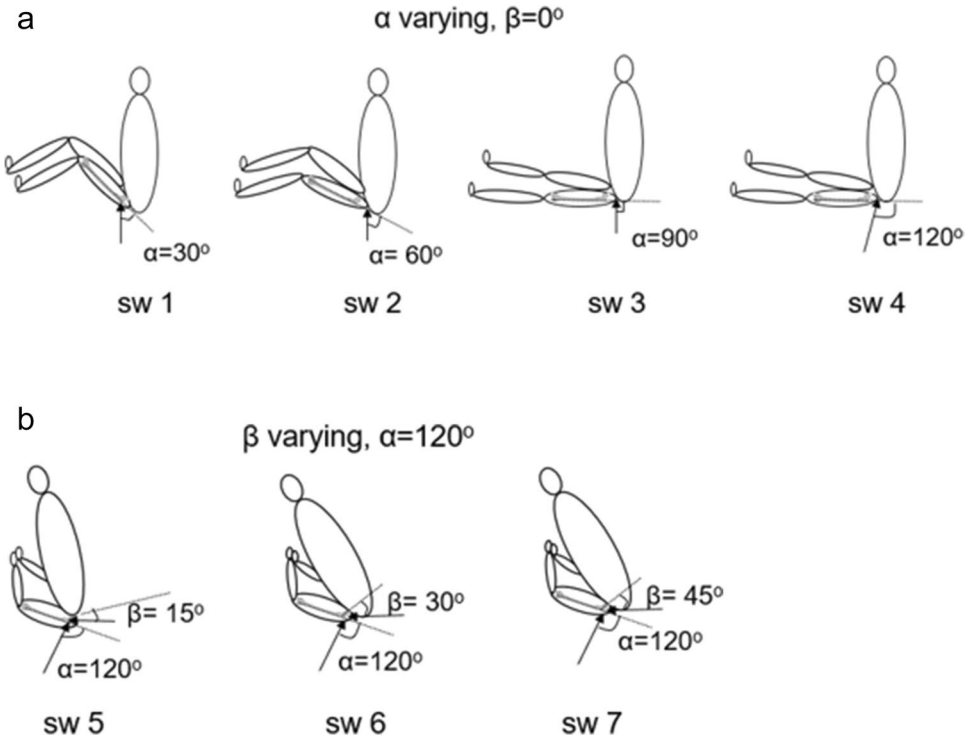

Fig. 2 Variation of fall loading direction **a** on coronal plane with respect to femoral shaft axis (α), while angle β is fixed at 0^o and **b** on transverse plane with reference to femoral neck axis (β) at a fixed angle α ($\alpha = 120^o$)

due to the contact with the acetabulum, physiologically, α is expected to vary between 0° and 180° with reference to femoral shaft, and β can vary from 0° to 90° with reference to the femoral neck axis on the transverse plane [1, 26]. However, prior investigation showed that the tendency to fracture is highest at α 120° and β 45° [1, 26, 42, 43]. Therefore, the maximum variations of angles α and β were limited to 120° on the coronal plane and 45° on the transverse plane in this current study (Fig. 2).

2.5 Bone morphology

The morphological parameters of the femur were measured from the 2D view of the meshed models of the left and right femurs of each patient on the coronal plane. As shown in Fig. 3, femoral shaft length (FSL)–AB was measured from the coordinates of the nodes of outer margin on the greater trochanter and distal condyle such that it passes through the middle of the femoral shaft; femoral neck width (FNW)–FG was calculated between the outer coordinates on the neck region, where it is minimum; femoral neck axis length (FNAL)–CD was obtained by considering the coordinate on the outer margin of the femoral head and greater trochanter such that it perpendicularly bisects the FNW; and femoral neck angle (FNA) is defined as the angle between FNAL and FSL [27]. The true moment arm (TMA)–ED is defined as the horizontal component of FNAL on the transverse plane [30].

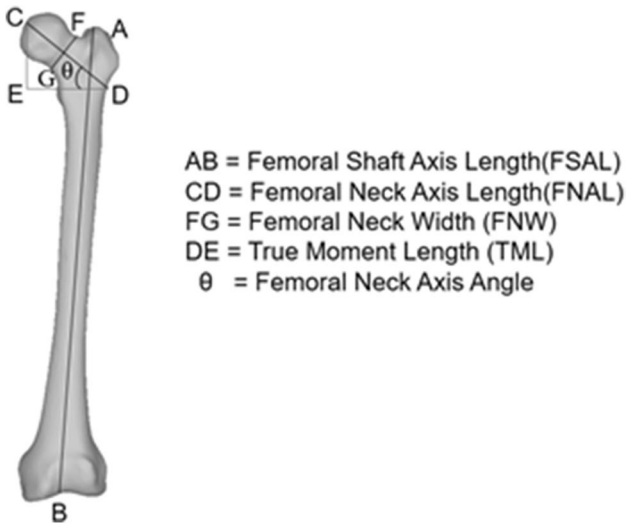

Fig. 3 Morphology of femur showing different geometric parameters considered in the statistical analysis

2.6 Failure criteria

A linear FEA was conducted in this study considering the femur has linear elastic behavior up to failure during loading conditions [44–46]. In addition, the femur resembles brittle behavior that may be well represented by the maximum stress–strain criteria than the von Mises stress and strain [47]. Prior studies considered either stress- [33, 48–51] or strain-based [52–55] analysis to predict fracture risk.

However, research [31, 56–58] showed that principal strain-based FEA could estimate the fracture risk more accurately over others. Hence, in this study, we adopted the maximum principal strain-based criteria to estimate the FRI, which is defined on the basis of maximum tensile strain and compressive strain in Eqs. (4) and (5) [31].

$$FRI = \frac{\varepsilon^{T}_{\max}}{0.0073} \tag{4}$$

$$FRI = \frac{|\varepsilon^{C}_{\max}|}{0.0104} \tag{5}$$

where $\varepsilon^{T}_{\max}$ and $\varepsilon^{C}_{\max}$ are the maximum principal strain in tension and compression, respectively.

2.7 Statistical analysis

The primary goal of this study was to investigate the extent to which different parameters influence femoral fracture based on the calculated FRI [31]. Therefore, to analyze the parametric significance and dependencies, a multiple regression model was developed using a statistical software JMP® Pro 15 (SAS Institute Inc., USA) considering different fall load directions α and β, age, gender, patient height, and bone morphology including FSL, FNAL, FNA, TML, and FNW as the independent parameters and FRI as the dependent parameter. To evaluate the significance of the independent parameters on FRI, analysis of variance (ANOVA) tests were conducted. Effect tests were conducted to investigate the influence of the parameters and their extent of impact on FRI as well.

3 Results

FE analyses were conducted in ANSYS v19.0 (Ansys, Inc., USA) to determine the strain-based FRI for different sideways fall scenarios, considering strain as the primary outcome of the simulation. The current study was verified for the sideways fall, where the loading direction is perpendicular to the shaft axis, similar to the sw 3 fall configuration (Fig. 2) against the study conducted by Kheirollahi et al. [35] with the patient subset of the same dataset. For both left and right femurs, the average maximum von Mises strain (*mean* ± *SD*) of the present work was compared with Kheirollahi et al. [35]. As observed, the maximum von Mises strain of the current work falls within the range of the prior study at FN and intertrochanteric (intT) regions (Fig. 4). However, no information is available if the same patients were considered for both studies. Furthermore, the prior study considered 10 clinical cases whereas the current study considers 30 patients from the same and larger dataset.

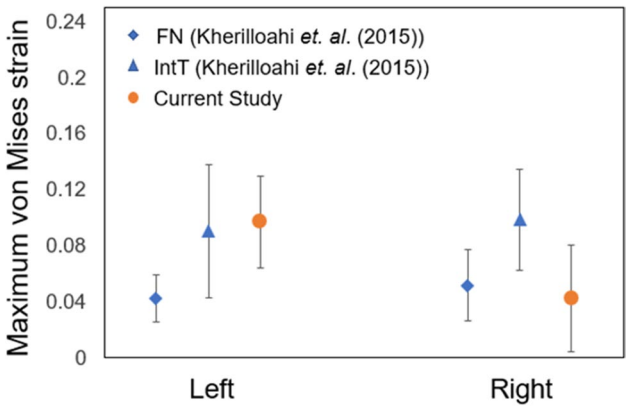

Fig. 4 Verification of current computational model against the study conducted by Kheirollahi et al. [35] by comparing the maximum von Mises strain for left and right femurs

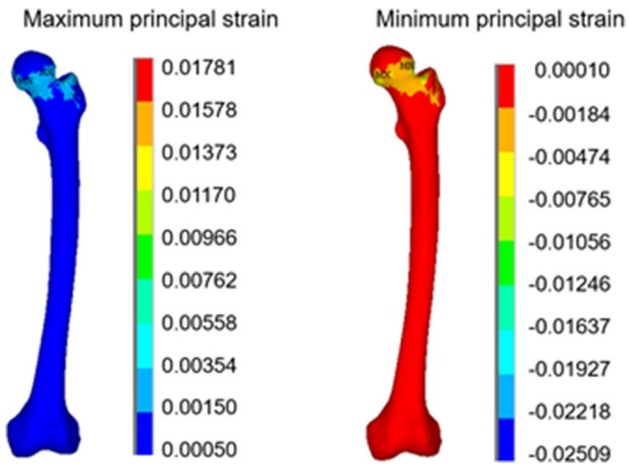

Fig. 5 An example of the distribution of maximum (**a**) and minimum (**b**) principal strain in a femur due to sideways fall condition where the loading direction is perpendicular to the shaft axis (sw 3). Higher principal strain has been observed in femoral neck region

Figure 5a shows the typical distributions of maximum (tensile) principal strain and Fig. 5b shows the minimum (compressive) principal strain in a femur. The strain distribution shows that the maximum strain is primarily evident at the proximal end of the femur including FN and trochanteric regions such as intertrochanteric (ITC), and sub-trochanteric regions. For the sideways fall loading, typically the superior aspect of the FN is compression whereas the inferior aspect is tension. Each femur was simulated with 7 different loading directions (Fig. 2), and the average variation of the maximum principal strain at each loading direction—mimicking a sideways fall posture—is shown in Fig. 6. It is evident that the principal strains are mostly affected by the fall orientation on the transverse plane (β) in comparison with the loading direction (α) on coronal plane. The maximum

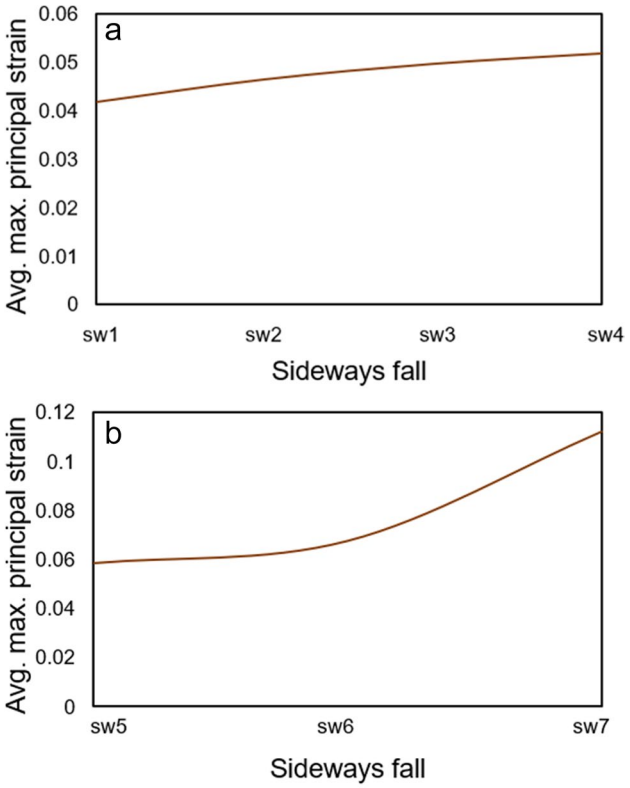

Fig. 6 Average variation of maximum principal strain in femoral neck region **a** at different loading angle α when β is fixed at 0°, and **b** at different loading angle β when α is constant at 120°. On changing loading direction α and β, the average maximum principal strain varies

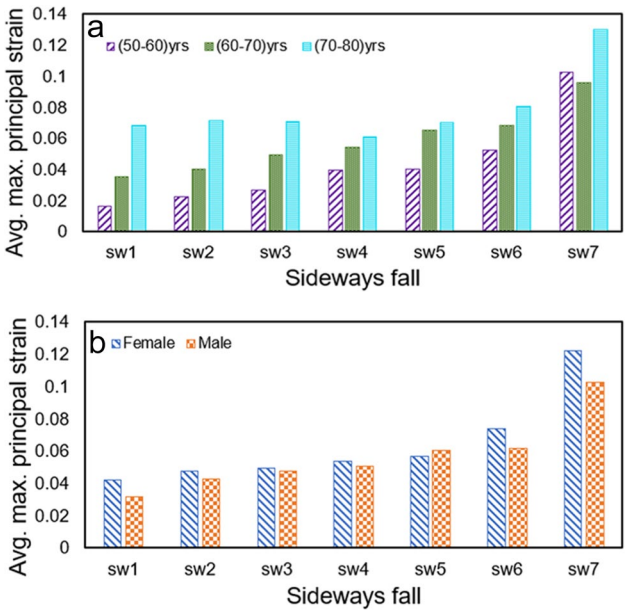

Fig. 7 Comparison of maximum principal strain between female and male (**a**) and among different age groups (**b**) during different sideways fall loading conditions

strain varied between 0.118 and 0.067 as α on the coronal plane changed from 30° to 120°, whereas the principal strain varies from 0.098 to 0.194 as β changes from 0° to 30° on the transverse plan. The maximum strain was observed and started declining as it passes beyond 30°. (Or observation of the maximum strain shows that it started declining as it passes beyond 30°.)

The variation of strain between male and female, and different age groups for different loading configurations are shown in Fig. 7. Principal strain in female is higher than that of male subjects irrespective of loading configurations (Fig. 7a). However, strain is considerably higher both in male and in female when loading direction makes larger angles ($\beta > 15^o$) on transverse plane. The larger principal strain is responsible for femoral fracture as well. The variation of principal strain among different age groups shows that with increasing age, the principal strain also increases, and it is higher when the loading direction on the transverse plane makes a larger angle with femoral neck axis. These results implicate that older females are more susceptible to hip fracture during the sideways fall than males [19, 20].

Table 2 shows the ANOVA test evaluating the significance of the independent parameters on FRI. The null hypothesis in this context means that there is no significance of parameters on FRI. The test statistic is the F value of 7.4478 when conducted F-test at 0.05 significance level. Since the p-value ($p < .0001$) for 7.4487 is less than 0.05, the null hypothesis is rejected and indicated that FRI depends on the independent parameters considered herein. The significance level of 0.05 also represents a 95% confidence level.

The ANOVA test determines the overall significance of the FRI, but it does not tell us which predictors (parameters) are more significant that may play critical roles over others when assessing fracture. Hence, the effect tests have been conducted to investigate the influence of the parameters and their extent of impact on FRI and the effect summary is shown in Table 3, which was generated based on a multiple regression model. The p-value ($p < 0.05$) for β, age, TML, gender, FNA, height, and FSL is shown to have high significance with 95% confidence level, while other parameters with a p-value greater than 0.05 are insignificant. LogWorth is adjusted p-value,

Table 2 ANOVA for individual parameters

Source	DF	Sum of squares	Mean square	F ratio
Model	11	8716.079	792.371	7.4478
Error	387	41,172.938	106.390	**Prob > *F***
C. total	398	49,889.018		<.0001

Table 3 Effect summary of individual parameters on FRI

Source	LogWorth	PValue
beta	5.503	0.0000
age	3.206	0.0006
TML	3.197	0.0006
gender	2.831	0.0015
FNA	1.674	0.0213
body height	1.623	0.0238
FSL	1.502	0.0315
weight	1.115	0.0767
FNW	0.346	0.4504
alpha	0.279	0.5258
FNAL	0.112	0.7719

Table 4 ANOVA for two-level interaction regression model

Source	DF	Sum of squares	Mean square	*F* ratio
Model	65	36,397.178	559.957	13.8206
Error	333	13,491.840	40.516	Prob > *F*
C. total	398	49,889.018		< .0001

defined as $\log 10(p - value)$, that provides an appropriate scale for graphing. LogWorth with a value of 1.301 and greater is significant at 0.05 significant level. The graphical representation of LogWorth also shows the priority of effect, i.e., ranking of independent parameters based on their critical influence on FRI.

A multiple regression model of two-level interaction was also developed to analyze the effect of the interaction of independent parameters on the FRI. The significance of two-level interaction on FRI was evaluated by ANOVA as shown in Table 4. The test statistic is the *F* value of 13.8206, when conducted the *F*-test at 0.05 significance level similar to the ANOVA of one-level independent parameter. The test statistic implies that FRI depends on the two-level interaction of independent parameters as well ($p < .0001$). To categorize which combinations of the parameters are more significant over others, effect tests were conducted along with the ANOVA test. The effect tests show the significance of each two-level interaction as the *p*-value ($p < .0001$) is less than 0.05, indicating the significance of interaction with a 95% confidence level (Table 5). However, due to a long list of two-level interaction between 11 independent parameters, only the interactions of the parameters that have significant effect on FRI have been shown on the LogWorth graph (Table 5).

A multiple regression model of three-level interaction was also conducted to evaluate the effect of three-level interaction on femoral fracture risk. The three-level interaction model shows that the effect of one parameter depends on the other two parameters. Table 6 represents the significance of three-level interaction on FRI evaluated by ANOVA. The *F* statistic with *p*-value ($p < .0001$) shows that FRI depends on three-level interaction. However, to prioritize the effect of the different combinations of the three interacting parameters, the effect tests were conducted and the LogWorth graph is shown in Table 7. The effect summary shows only those parameters having *p*-value less than a significance level 0.05 (Table 7).

4 Discussion

The primary goal of this study is to statistically analyze the effect of different bone morphological and physiological parameters that may have strong correlation with the fracture risk of a femur. Based on prior studies [2, 25–27], 11 different parameters—loading directions denoted by α and β, age, gender, patient height, weight, and bone morphology such as FSL, FNAL, FNA, TML, and FNW—were considered the probable influential parameters for fracture risk assessment in the current study. The maximum principal strain for 30 pairs of femurs was simulated with 7 different loading directions to calculate their respective FRIs. A multiple regression model was eventually developed to find the significance

Table 5 Effect summary of parameters on FRI with two-level interaction

Source	LogWorth	PValue
gender*FSL	12.898	0.0000
FNAL*TML	11.036	0.0000
gender*body height	10.950	0.0000
age*weight	6.592	0.0000
body height*FNW	5.322	0.0000
body height*FSL	5.238	0.0000
age*gender	4.721	0.0000
gender*TML	4.666	0.0000
FNA*TML	4.595	0.0000
gender*FNA	4.071	0.0001
FNW*FSL	3.996	0.0001
weight*FNA	3.980	0.0001
weight*FNAL	3.871	0.0001
weight*TML	3.810	0.0001
gender	3.774	0.0002
gender*FNAL	3.668	0.0002
weight	3.439	0.0004
FNAL	3.095	0.0008
weight*FSL	2.991	0.0010
FNA	2.684	0.0021
FSL*TML	2.487	0.0033
TML	2.471	0.0034
FSL*FNAL	2.450	0.0036
FSL*FNA	2.420	0.0038
FSL	2.247	0.0057
FNW	2.194	0.0064
body height*FNA	2.155	0.0070
age	2.152	0.0070
Source	**LogWorth**	**PValue**
age*FNAL	2.144	0.0072
FNW*TML	2.105	0.0079
body height*TML	2.104	0.0079
body height*FNAL	2.078	0.0084

Table 6 ANOVA for three-level interaction regression model

Source	DF	Sum of squares	Mean square	*F* ratio
Model	154	46,674.069	303.078	23.0023
Error	244	3214.949	13.176	Prob > *F*
C. total	398	49,889.018		< .0001

between the independent parameters and dependent parameter—FRI—and its effect tests was performed to analyze the degree of impact along with two-level and three-level interactions. One of the major advantages of this analysis is the ability to categorize the independent parameters based on their influence on the femoral fracture. It will also help us determine the dependency of parameters or the effect of the interaction of the parameters that may influence the FRI as well.

Among all the fractures observed in different locations of a femur, 60% of total fractures are FN fracture [59]. Fractures at FN and ITC are often the consequence of fall from patients' standing height on the greater trochanter, whereas sub-trochanteric fractures generally occur due to high impact energy originating from major or fatal accidents [60]. The strain distributions (Fig. 5) show that the maximum and minimum principal strain are also observed at the inferior and superior surface of femoral neck, respectively. The higher strain distributions on the femoral neck region suggest the vulnerability of fracture in that region during the sideways fall [18, 35] which are also observed clinically [61]. The variation of maximum principal strain largely depends on loading directions (Fig. 6). It is inferred from the analysis that angle β on the transverse plane plays a critical role compared to angle α on the coronal plane, especially when β forms an angle greater than 30^o with the femoral neck axis. These results further imply that the femur is the weakest at certain sideways falling posture.

The high susceptibility of femoral fracture in female over male (Fig. 7a) may be due to the deterioration of bone density being greater in a female than in a male [7]. The increase in strain value with age (Fig. 7b) depicts the physiological fact that bone loss occurs with age. These results have clinical relevance, because older people and females are more prone to osteoporotic fracture as observed clinically. Furthermore, we often observe osteoporotic fracture in aged females as they mostly suffer from osteoporosis due to bone loss, which is often influenced, among others, by the imbalance of sex hormones especially after menopause.

It is evident that patient physiology and femur morphology coupled with mechanical loading have a cumulative effect on FRI but assessing their role in order of their severity has not been done explicitly to the best of our knowledge. The unique contribution of this work is to categorize the eleven parameters, considered herein, allowing their individual and combined (two- and three-level interactions) effect on FRI based on the LogWorth graph and/or the quantitative significance *p*-value of the parameters (Tables 3, 4, 5).

The effect tests on individual parameters categorize their significance based on their isolated effect, which are reflected by the *p*-values and LogWorth graph (Table 2). For instance, the effect tests of loading direction shows that β is significant ($p < 0.05$), but not $\alpha (p > 0.05)$ at significance level 0.05, meaning that the loading direction on the transverse plane with reference to femoral neck axis (β) has greater effect on fracture risk with 95% confidence level in comparison with α on the coronal plane. This signifies that a fracture is more likely to take place when someone's fall posture makes a greater angle with the femoral neck axis on the transverse plane. However, it is not possible to control sudden free-fall posture, but it indicates loading direction plays a vital role in triggering the hip fracture. In addition to *p*-value, the LogWorth value helps us to easily identify the significance of those parameters as well. The effect tests as well as the LogWorth values show that physiological parameters such age ($p < 0.0006$), gender ($p < 0.0015$), FNA ($p < 0.0213$), height ($p < 0.0238$), and FSL ($p < 0.0315$) have greater significance compared to weight indicating that the probability of hip fracture increases with an increase in this individual parameter. Similarly, the significance of morphological parameters is also observed. For example, TML ($p < 0.0006$) has much higher impact than FNA ($p < 0.0212$). Among the considered 11 parameters, individually the morphological parameters—FNW and FNAL—and physiological parameters such as weight are found insignificant in addition to loading direction α. Therefore, we can assume that the isolated changes in these parameters may not significantly contribute to the hip fracture. The insignificance of FNAL was also observed

Table 7 Effect summary of parameters on FRI with three-level interaction

Source	LogWorth		PValue
beta*FNAL*FNA	2.188		0.0065
beta*FNAL*TML	2.183		0.0066
beta*age*FNW	2.099		0.0080

in prior studies made by Fajar et al. [27, 62]. However, the insignificance of FNW contradicts with prior observation [27, 30], which may be due to the variations in sample size, age, level of osteoporosis, and ethnicity.

Identifying the categorical significance of individual parameters is important as it will provide an insight into design and develop preventive mechanisms, but these parameters work synergistically, and therefore, the significance of interaction of parameters has also been conducted (Table 4). The result of the ANOVA test in Table 4 also shows the significance of two-level interaction—the effect of one parameter on hip fracture depending on other parameters. For instance, the interaction of sex and femur length represented by gender × FSL in Table 5 contributes the most in hip fracture, meaning the effect of sex on fracture risk depends on the patient's femur length. This implies that people of the same sex may be assessed with different fracture risk probability if their femur lengths are different. After gender × FSL, the high significant interaction is FNAL × TML. The significance of the combined effect of FNAL × TML shows one important conclusion that the individually insignificant parameters (e.g., FNAL, weight in Table 3) may exhibit higher significance such as FNAL × TML ($p < 0.0000$) while interacting with each other in synergy. Based on the Log-Worth values, we can easily identify which combinations of the parameters are more significant in affecting fracture when they interact with each other. However, it should be noted that only the significant ($p < 0.05$) two-level interactions are shown in Table 5 but not the others. Similarly, the significance of three-level interaction shown in Table 7 delineates that the parameter interacts with more than two parameters also affecting fracture risk. As observed, very few (only 3) parameters exhibit significance in this three-level interaction (Table 7). Other three-level interactions were not shown in Table 7 as they were found insignificant.

There are some limiting assumptions in this study and may impact computational results. First, we varied the angle α and β by 4 discrete intervals between the limits that we considered and the variation of α was conducted keeping β fixed and vice versa. Varying both α and β simultaneously may provide better insights into the effect of the loading directions on fracture risk assessment. Second, the significance of interaction was limited up to three-level interaction. The higher-level interactions were omitted due to the lost degree of freedom and a long list of interacting parameters. Next, muscle effect was not considered even though it acts as an energy absorber, reducing the loading impact, which contributes shear stress at the muscle-bone interface. However, the computational model was primarily designed in such a way that ex vivo experiments can be designed to validate the FE outcomes. Finally, bone density was not considered an independent parameter because 90% of patient studied herein were found with healthy bones and non-osteoporotic, according to the *T*-score value provided by WHO. Considering BMD as an insignificant parameter due to non-osteoporotic patient cohorts herein, the study specifically aims at analyzing the parameter that impacts femoral fracture on healthy bone and the selection of parameters was done in accordance with prior studies [7, 63].

5 Conclusions

The primary goal of this work was to assess the hip fracture risk considering parameters associated with patient physiology, bone morphology, and the mechanics of fall. Therefore, we investigated the quantitative significance of the parameters on FRI to prioritize them individually and their two-level and three-level interaction among the parameters. The multiple regression analysis, considering fall posture, patient physiology, and bone morphology as independent parameters and FEA, derived FRI as a dependent parameter. One-level interaction showed that all parameters are not statistically significant and the parameters that are significant may not have equal emphasis on FRI. However, higher-level interactions showed that the combinations of insignificant parameters may have higher significance in influencing the hip fracture. The significance of two-level and three-level interaction further showed that the effect of one parameter on femoral fracture risk is not always constant rather it depends on the other parameters. To the best of our knowledge, no prior work attempted to rank the order of influential parameters in fracture risk assessment. Hence, this study gives an insight into the fact that not all the parameters are equally important, and their combined effect may differ significantly than the isolated parameters. Therefore, analyzing the importance of parameters and their interactions could help assess better fracture risk, and thereby develop effective preventing measures to avoid hip fracture of elderly population.

Acknowledgements The authors greatly appreciate the contribution of Dr. Hossein Kheirollahi in medical image processing. The authors also appreciate the help of John Carroll, a Ph.D. candidate at UL Lafayette, for the language editing service.

References

1. Lee Y, Ogihara N, Lee TJ (2019) Assessment of finite element models for prediction of osteoporotic fracture. J Mech Behav Biomed Mater 97:312–320
2. Szulc P, Marchand F, Duboeuf F, Delmas PJ (2000) Cross-sectional assessment of age-related bone loss in men: the MINOS study. Bone 26(2):123–129
3. Bettamer A (2013) prediction of proximal femur fracture: finite element modeling based on mechanical damage and experimental validation.

4. Group RoaWS (1994) Assessment of fracture risk and its application to screening for postmenopausal osteoporosis. HO Technical Report Series, vol 843. World Health Organization, Geneva
5. Organization WH WHO scientific group on the assessment of osteoporosis at primary health care level: summary meeting report 2004. Belgium WHO:5–7
6. Johnell O, Kanis JA, Oden A, Johansson H, De Laet C, Delmas P, Eisman JA, Fujiwara S, Kroger H, Mellstrom DJ (2005) Predictive value of BMD for hip and other fractures. J Bone Miner Res 20(7):1185–1194
7. Tenenhouse A, Joseph L, Kreiger N, Poliquin S, Murray T, Blondeau L, Berger C, Hanley D, Prior J, International CRG (2000) Estimation of the prevalence of low bone density in Canadian women and men using a population-specific DXA reference standard: the Canadian Multicentre Osteoporosis Study (CaMos). Osteoporos Int 11(10):897–904
8. Beck TJ, Oreskovic TL, Stone KL, Ruff CB, Ensrud K, Nevitt MC, Genant HK, Cummings SR (2001) Structural adaptation to changing skeletal load in the progression toward hip fragility: the study of osteoporotic fractures. J Bone Miner Res 16(6):1108–1119
9. Ferizi U, Besser H, Hysi P, Jacobs J, Rajapakse CS, Chen C, Saha PK, Honig S, Chang GJ (2019) Artificial intelligence applied to osteoporosis: a performance comparison of machine learning algorithms in predicting fragility fractures from MRI data. J Magn Reson Imaging 49(4):1029–1038
10. Luo Y, Ferdous Z, Leslie W (2011) A preliminary dual-energy X-ray absorptiometry-based finite element model for assessing osteoporotic hip fracture risk. Proc Inst Mech Eng [H] 28:1188–1195
11. Ahlborg HG, Nguyen ND, Nguyen TV, Center JR, Eisman JA (2005) Contribution of hip strength indices to hip fracture risk in elderly men and women. J Bone Miner Res 20(10):1820–1827
12. Beck TJ, Ruff CB, Warden KE, Scott WW Jr, Rao GU (1990) Predicting femoral neck strength from bone mineral data: a structural approach. Invest Radiol 25(1):6–18
13. Mourtada FA, Beck TJ, Hauser DL, Ruff CB, Bao GJ (1996) Curved beam model of the proximal femur for estimating stress using dual-energy x-ray absorptiometry derived structural geometry. J Orthop Res 14(3):483–492
14. Keyak JH, Kaneko TS, Tehranzadeh J, Skinner HB (2005) Predicting proximal femoral strength using structural engineering models. Clin Orthop Relat Res 437:219–228
15. Duchemin L, Bousson V, Raossanaly C, Bergot C, Laredo J, Skalli W, Mitton D (2008) Prediction of mechanical properties of cortical bone by quantitative computed tomography. Med Eng Phys 30(3):321–328
16. Bauer J, Kohlmann S, Eckstein F, Mueller D, Lochmüller E-M, Link T (2006) Structural analysis of trabecular bone of the proximal femur using multislice computed tomography: a comparison with dual X-ray absorptiometry for predicting biomechanical strength in vitro. Calcif Tissue Int 78(2):78–89
17. Ohnaru K, Sone T, Tanaka K, Akagi K, Ju Y-I, Choi H-J, Tomomitsu T, Fukunaga M (2013) Hip structural analysis: a comparison of DXA with CT in postmenopausal Japanese women. Sringerplus 2(1):331
18. Faisal TR, Luo Y (2017) Study of the variations of fall induced hip fracture risk between right and left femurs using CT-based FEA. Biomed Eng Online 16(1):116
19. Luo Y, Ferdous Z, Leslie W (2011) A preliminary dual-energy X-ray absorptiometry-based finite element model for assessing osteoporotic hip fracture risk. Proc Inst Mech Eng H 225(12):1188–1195
20 Wiktorowicz M, Goeree R, Papaioannou A, Adachi JD, Papadimitropoulos E (2001) Economic implications of hip fracture: health service use, institutional care and cost in Canada. Osteoporos Int 12(4):271–278
21. Ariza OR (2010) A novel approach to finite element analysis of hip fractures due to sideways falls. University of Waterloo
22. Cody DD, Gross GJ, Hou FJ, Spencer HJ, Goldstein SA, Fyhrie DP (1999) Femoral strength is better predicted by finite element models than QCT and DXA. J Biomech 32(10):1013–1020
23 Marks R, Allegrante JP, MacKenzie CR, Lane JM (2003) Hip fractures among the elderly: causes, consequences and control. Ageing Res Rev 2(1):57–93
24. Esses SI, Lotz JC, Hayes WC (1989) Biomechanical properties of the proximal femur determined in vitro by single-energy quantitative computed tomography. J Bone Miner Res 4(5):715–722
25. Pinilla T, Boardman K, Bouxsein M, Myers E, Hayes W (1996) Impact direction from a fall influences the failure load of the proximal femur as much as age-related bone loss. Calcif Tissue Int 58(4):231–235
26 Ford CM, Keaveny TM, Hayes WC (1996) The effect of impact direction on the structural capacity of the proximal femur during falls. J Bone Miner Res 11(3):377–383
27. Fajar JK, Taufan T, Syarif M, Azharuddin A (2018) Hip geometry and femoral neck fractures: a meta-analysis. J Orthop Transl 13:1–6
28. Faisal TR, Luo Y (2016) Study of stress variations in single-stance and sideways fall using image-based finite element analysis. Bio-Med Mater Eng 27(1):1–14
29. Keller TS (1994) Predicting the compressive mechanical behaviour of bone. J Blomechanics 29:1159–1168
30. Gong H, Zhang M, Fan Y, Kwok WL, Leung PC (2012) Relationships between femoral strength evaluated by nonlinear finite element analysis and BMD, material distribution and geometric morphology. Ann Biomed Eng 40(7):1575–1585
31. Schileo E, Taddei F, Cristofolini L, Viceconti MJ (2008) Subject-specific finite element models implementing a maximum principal strain criterion are able to estimate failure risk and fracture location on human femurs tested in vitro. J Biomech 41(2):356–367
32 Ashman R, Van Buskirk W (1987) The elastic properties of a human mandible. Adv Dent Res 1(1):64–67
33. Keyak JH, Rossi SA, Jones KA, Skinner HB (1997) Prediction of femoral fracture load using automated finite element modeling. J Biomech 31(2):125–133
34. Lotz J, Cheal E, Hayes WC (1991) Fracture prediction for the proximal femur using finite element models: part II—nonlinear analysis. J Biomech Eng
35. Kheirollahi H, Luo Y (2015) Assessment of hip fracture risk using cross-section strain energy determined by QCT-based finite element modeling. BioMed Res Int
36. Faisal TR, Luo Y (2016) Study of stress variations in single-stance and sideways fall using image-based finite element analysis. BioMed Res Int 27(1):1–14
37. Eckstein F, Wunderer C, Boehm H, Kuhn V, Priemel M, Link TM, Lochmüller EM (2004) Reproducibility and side differences of mechanical tests for determining the structural strength of the proximal femur. J Bone Miner Res 19(3):379–385
38. Nishiyama KK, Gilchrist S, Guy P, Cripton P, Boyd SK (2013) Proximal femur bone strength estimated by a computationally fast finite element analysis in a sideways fall configuration. J Biomech 46(7):1231–1236
39. Manske S, Liu-Ambrose T, De Bakker P, Liu D, Kontulainen S, Guy P, Oxland T, McKay H (2006) Femoral neck cortical geometry measured with magnetic resonance imaging is associated with proximal femur strength. Osteoporos Int 17(10):1539–1545
40. Yoshikawa T, Turner C, Peacock M, Slemenda C, Weaver C, Teegarden D, Markwardt P, Burr D (1994) Geometric structure of the femoral neck measured using dual-energy X-ray absorptiometry. J Bone Miner Res 9(7):1053–1064
41. Falcinelli C, Schileo E, Balistreri L, Baruffaldi F, Bordini B, Viceconti M, Albisinni U, Ceccarelli F, Milandri L, Toni A (2014)

Multiple loading conditions analysis can improve the association between finite element bone strength estimates and proximal femur fractures: a preliminary study in elderly women. Bone 67:71–80
42. van den Munckhof S, Zadpoor AA (2014) How accurately can we predict the fracture load of the proximal femur using finite element models? Clin Biomech 29(4):373–380
43 Awal R, Faisal TR (2021) Multiple regression analysis of hip fracture risk assessment via finite element analysis. J Eng Sci Med Diagn Ther 4(1):011006
44 Grassi L, Schileo E, Taddei F, Zani L, Juszczyk M, Cristofolini L, Viceconti M (2012) Accuracy of finite element predictions in sideways load configurations for the proximal human femur. J Biomech 45(2):394–399
45 Juszczyk MM, Cristofolini L, Viceconti M (2011) The human proximal femur behaves linearly elastic up to failure under physiological loading conditions. J Biomech 44(12):2259–2266
46 Cristofolini L, Juszczyk M, Martelli S, Taddei F, Viceconti M (2007) In vitro replication of spontaneous fractures of the proximal human femur. J Biomech 40(13):2837–2845
47 Doblaré M, Garcıa J, Gómez MJ (2004) Modelling bone tissue fracture and healing: a review. Eng Fract Mech 71(13–14):1809–1840
48. Marco M, Giner E, Caeiro-Rey JR, Miguélez MH, Larraínzar-Garijo R (2019) Numerical modelling of hip fracture patterns in human femur. Comput Methods Programs Biomed 173:67–75
49. Keyak J, Sigurdsson S, Karlsdottir G, Oskarsdottir D, Sigmarsdottir A, Zhao S, Kornak J, Harris T, Sigurdsson G, Jonsson B (2011) Male–female differences in the association between incident hip fracture and proximal femoral strength: a finite element analysis study. Bone 48(6):1239–1245
50. Keyak J, Sigurdsson S, Karlsdottir G, Oskarsdottir D, Sigmarsdottir A, Kornak J, Harris T, Sigurdsson G, Jonsson B, Siggeirsdottir K (2013) Effect of finite element model loading condition on fracture risk assessment in men and women: the AGES-Reykjavik study. Bone 57(1):18–29
51. Keaveny TM, Kopperdahl DL, Melton LJ III, Hoffmann PF, Amin S, Riggs BL, Khosla S (2010) Age-dependence of femoral strength in white women and men. J Bone Miner Res 25(5):994–1001
52 Bayraktar HH, Morgan EF, Niebur GL, Morris GE, Wong EK, Keaveny TM (2004) Comparison of the elastic and yield properties of human femoral trabecular and cortical bone tissue. J Biomech 37(1):27–35
53. Luo Y, Ferdous Z, Leslie WD (2013) Precision study of DXA-based patient-specific finite element modeling for assessing hip fracture risk. Int J Numer Methods Biomed Eng 29(5):615–629
54. Viceconti M, Davinelli M, Taddei F, Cappello A (2004) Automatic generation of accurate subject-specific bone finite element models to be used in clinical studies. J Biomech 37(10):1597–1605
55. Wakao N, Harada A, Matsui Y, Takemura M, Shimokata H, Mizuno M, Ito M, Matsuyama Y, Ishiguro N (2009) The effect of impact direction on the fracture load of osteoporotic proximal femurs. Med Eng Phys 31(9):1134–1139
56 Anderson AE, Peters CL, Tuttle BD, Weiss JA (2005) Subject-specific finite element model of the pelvis: development, validation and sensitivity studies. J Biomech Eng 127(3):364–373
57 Barker D, Netherway DJ, Krishnan J, Hearn TC (2005) Validation of a finite element model of the human metacarpal. Med Eng Phys 27(2):103–113
58. Gupta S, Van Der Helm F, Sterk J, Van Keulen F, Kaptein B (2004) Development and experimental validation of a three-dimensional finite element model of the human scapula. Proc Inst Mech Eng H 218(2):127–142
59 Basso T, Klaksvik J, Syversen U, Foss OA (2012) Biomechanical femoral neck fracture experiments—a narrative review. Injury 43(10):1633–1639
60. Ariza OR (2014) A novel approach to finite element analysis of hip fractures due to sideways falls. University of British Columbia
61 Röder F, Schwab M, Aleker T, Mörike K, Thon KP, Klotz U (2003) Proximal femur fracture in older patients–rehabilitation and clinical outcome. Age Ageing 32(1):74–80
62. Fajar JK, Taufan T, Syarif M, Azharuddin A (2018) Hip geometry and femoral neck fractures: A meta-analysis. J Orthop Translat 13:1–6
63. Liu Y-L, Hsu J-T, Shih T-Y, Luzhbin D, Tu C-Y, Wu J (2018) Quantification of volumetric bone mineral density of proximal femurs using a two-compartment model and computed tomography images. BioMed Res Int

Rabina Awal Rabina Awal is a Ph.D. student in the Department of Mechanical Engineering at the University of Louisiana at Lafayette. Her research focuses on assessing hip fracture risk using experiments and computational tools. Her expertise on computational modeling includes finite element modeling, machine learning, and computer vision.

Jalel Ben Hmida Dr. Jalel Ben Hmida is a professor of practice in Mechanical Engineering at the University of Louisiana at Lafayette. His research interests include optimization of large-scale systems, artificial intelligence, data analytics and statistics.

Yunhua Luo Dr. Yunhua Luo is a professor at the University of Manitoba and the Director of the Laboratory of Computational and Experimental Biomechanics. He has been conducting research on developing finite element algorithms and image-based biomechanical models to deal with computational challenges in biomechanical modeling of human-body injuries and the development of biomechanical tools to assess the risk of hip fracture.

Tanvir Faisal Dr. Tanvir Faisal is an assistant professor at the University of Louisiana at Lafayette and the Principal Investigator of the Musculoskeletal Mechanics and Multiscale Materials (4M) Laboratory. His research focuses on computational and experimental biomechanics especially in the areas of orthopedic biomechanics. His research goal is to understand the root cause of osteoporotic fracture and cartilage and knee mechanics in the context of osteoarthritis.